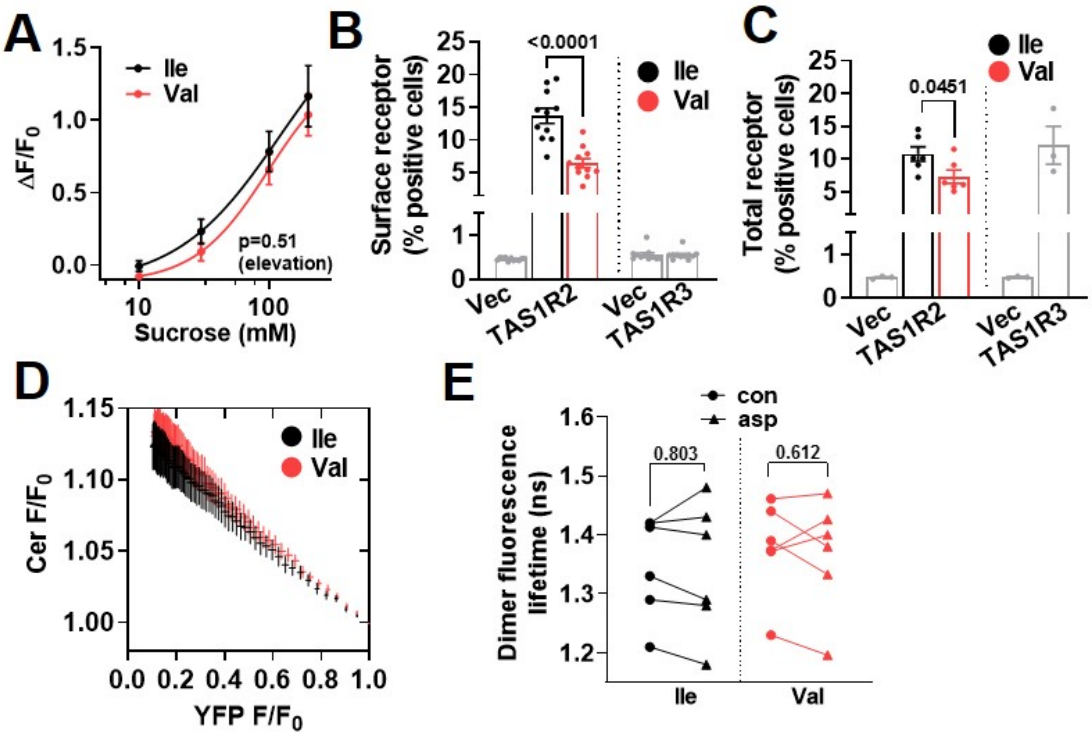

Supplemental Figure 1. The *TAS1R2*-(Val) variant reduces plasma membrane availability of STR dimer. **A)** Calcium mobilization in response to sucralose concentrations in transfected HEK293 cells with TAS1R2-(Ile) or TAS1R2-(Val) along with TAS1R3 and Gα16-gust44 (n=3, 30 cells). **B)** Flow cytometry analysis of surface protein expression of TAS1R2 (left bars) and TAS1R3 (right bars) shown as normalized percent positive cells in Expi293F cells transfected with FLAG–TAS1R2 constructs (Ile or Val) alone or Myc-TAS1R3 alone. Vec, vector-only control. **C)** Analysis of total protein expression of TAS1R2 (left bars) and TAS1R3 (right bars) shown as normalized percent positive cells in permeabilized Expi293F cells expressing FLAG–TAS1R2 constructs (Ile or Val) alone or Myc-TAS1R3 alone. **D)** Comparison of donor and acceptor relative fluorescence intensities for the assessment of linearity between Cer/YFP (data replotting from Figure1.D). **E)** Single spot lifetime acquisition (ns) for the TAS1R2-(Ile)/TAS1R3 and TAS1R2-(Val)-TAS1R3 dimers before and after the addition of aspartame indicative of the donor-acceptor distance of the complexes. Con, control; asp, after aspartame. Linear regression (A); t-test (B,C); Paired t-test (E).

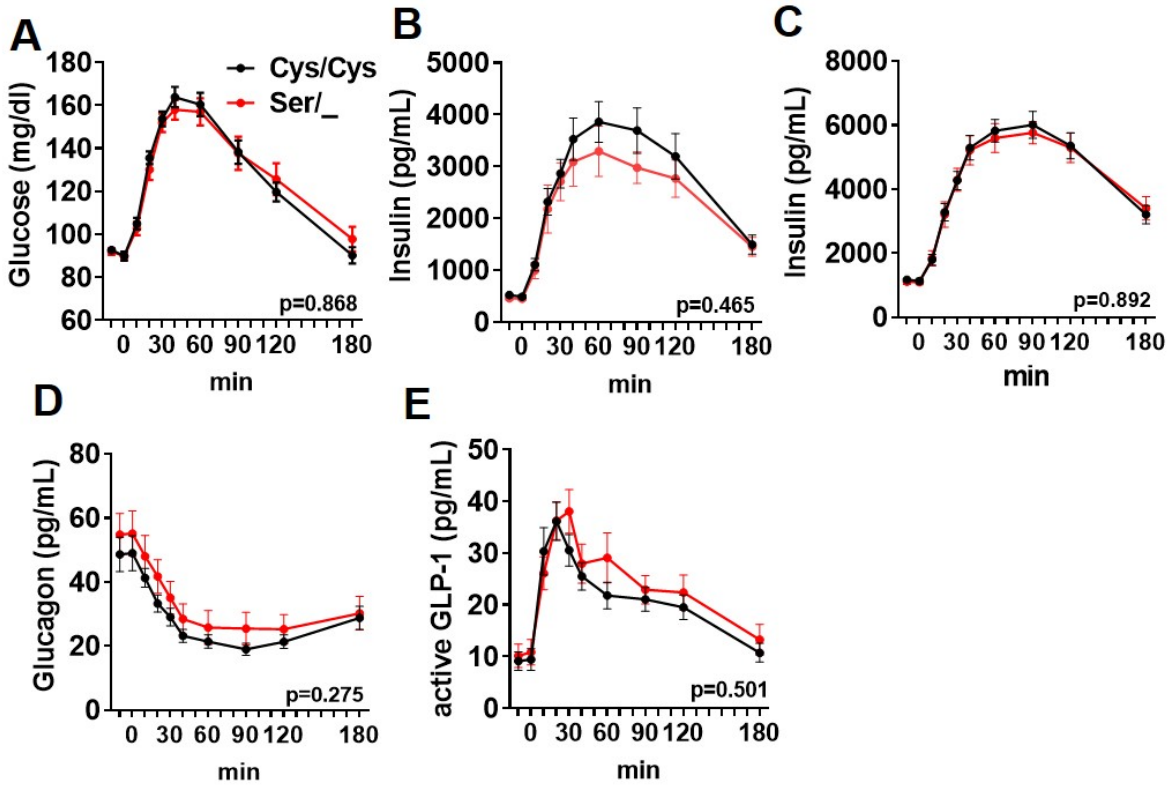

Supplemental Figure 2. The *TAS1R2* Ser9Cys variant is not associated with reduced glucose excursions in humans. Plasma excursions of **(A)** glucose, **(B)** insulin, **(C)** C-peptide, **(D)** glucagon, and **(E)** active GLP-1 in response to an oral glucose challenge in healthy lean Ser/Ser and Cys carriers with normal glucose control (n=16-30/group). Two-way ANOVA repeated measures, p-value of time x genotype effect.

Supplemental Table.1

Allele frequency, distribution and linkage

	Allele Frequency	χ^2	P
Hardy Weinberg			
Ile/Ile	26 (57%)		
Ile/Val	17 (37%)	0.094	0.954
Val/Val	3 (7%)		
Hardy Weinberg			
Cys/Cys	30 (65%)		
Ser/Cys	15 (33%)	0.346	0.841
Ser/Ser	1 (2%)		
Allele distribution (Ile191Val)			
*Recorded (n=216414)			
Ile	68%	1.202	0.273
Val	32%		
Observed (n=46)			
Ile	75%		
Val	25%		
Allele distribution (Ser9Cys)			
*Recorded (n=114744)			
Cys	78%	0.707	0.480
Ser	22%		
Observed (n=46)			
Cys	82%		
Ser	18%		
Linkage between SNPs		0.001	0.978

P values for Hardy-Weinberg equilibrium and allele distribution were obtained using chi square test. Linkage was obtained using chi square for association.

*L. Phan, Y. Jin, H. Zhang, W. Qiang, E. Shekhtman, D. Shao, D. Revoe, R. Villamarin, E. Ivanchenko, M. Kimura, Z. Y. Wang, L. Hao, N. Sharopova, M. Bihan, A. Sturcke, M. Lee, N. Popova, W. Wu, C. Bastiani, M. Ward, J. B. Holmes, V. Lyoshin, K. Kaur, E. Moyer, M. Feolo, and B. L. Kattman. "ALFA: Allele Frequency Aggregator." National Center for Biotechnology Information, U.S. National Library of Medicine, 10 Mar. 2020, www.ncbi.nlm.nih.gov/snp/docs/gsr/alfa/.

Supplemental Table.2

Microbial diversity in a cohort of healthy lean adults grouped by two common *TAS1R2* polymorphisms.

	Ile/Ile	**Val/_**	***P***	**Ser/_**	**Cys/Cys**	***P***
alpha diversity						
Family						
chao	38.79 ± 0.65	40.11 ± 1.03	*0.269*	40.43 ± 1.18	38.86 ± 0.64	*0.213*
shannon	2.79 ± 0.02	2.80 ± 0.03	*0.823*	2.82 ± 0.03	2.78 ± 0.02	*0.358*
simpson	0.90 ± 0.00	0.90 ± 0.01	*0.897*	0.90 ± 0.01	0.90 ± 0.00	*0.688*
Genus						
chao	70.21 ± 1.12	69.75 ± 1.55	*0.809*	71.07 ± 1.87	69.49 ± 1.03	*0.427*
shannon	3.43 ± 0.02	3.46 ± 0.03	*0.393*	3.48 ± 0.03	3.42 ± 0.02	*0.188*
simpson	0.95 ± 0.00	0.95 ± 0.00	*0.586*	0.95 ± 0.00	0.95 ± 0.00	*0.403*
beta diversity						
	PERMANOVA (Ile/Ile vs. Val/_)			PERMANOVA (Ser/Ser vs. Cys/_)		
Family						
F-value		0.71			0.89	
R^2		0.02			0.02	
P		< 0.740			< 0.571	
Genus						
F-value		1.03			0.82	
R^2		0.02			0.02	
P		< 0.420			< 0.685	

All values are mean ± SEM. Alpha diversity was assessed using three different indexes (chao, shannon, simpson). P value for genotype effect was obtained using t-tests. Beta diversity was assessed using PERMANOVA. Diversity was calculated for the Family and Genus taxonomic levels.

Supplemental Table.3

Unbiased associations of rs35874116 with type 2 diabetes traits in phenome-wide association studies (PheWAS)

Phenotype	Group	P-Value	Beta	Odds Ratio	Sample Size
Ascending aorta diameter	CARDIOVASCULAR	0.0140	▲0.0147		33,420
Disposition index adj BMI	GLYCEMIC	0.0268	▲0.0585		4,718
Two-hour C-peptide	GLYCEMIC	0.0282	▲0.6109		546
Type 1 diabetes	GLYCEMIC	0.0453		▲1.0290	57,284
Serum ApoB	LIPIDS	0.0185	▲0.0327		14,459
Dyslipidemia	LIPIDS	0.0396		▲1.0283	56,375
Triglyceride-to-HDL ratio	LIPIDS	0.0491	▼-0.0123		32,534
Citrate	METABOLITE	0.0088	▲0.0406		10,973
Beta-hydroxybutyric acid	METABOLITE	0.0395	▲0.0327		10,349
Vitamin D	NUTRITIONAL	0.0016	▼-0.0832		3,558
Neovascular age-related macular degeneration	OCULAR	0.0037		▲1.1935	2,786
Age-related macular degeneration	OCULAR	0.0420		▲1.0576	13,780
Late diabetic kidney disease adj HbA1c-BMI	RENAL	0.0008		▲1.1153	9,298
All diabetic kidney disease adj HbA1c-BMI	RENAL	0.0012		▲1.0904	18,103
Macroalbuminuria vs. controls	RENAL	0.0015		▲1.1055	9,268
Macroalbuminuria vs. controls adj HbA1c-BMI	RENAL	0.0021		▲1.1294	8,968
Chronic kidney disease and diabetic kidney disease adj HbA1c-BMI	RENAL	0.0149		▲1.1082	14,039
End-stage renal disease in type 2 diabetes	RENAL	0.0185		▲1.7390	300
Albuminuria in type 2 diabetes	RENAL	0.0284		▼0.9125	1,691
Microalbuminuria in type 2 diabetes	RENAL	0.0454		▼0.9063	1,201
Relative amplitude	SLEEP AND CIRCADIAN	0.0121	▲0.0008		160,686
Chronotype (binary sMEQ score)	SLEEP AND CIRCADIAN	0.0236		▲1.0943	6,449
Chronotype (continuous sMEQ score)	SLEEP AND CIRCADIAN	0.0455	▼-0.1483		7,436
Mean sleep duration, rank-normalized	SLEEP AND CIRCADIAN	0.0460	▼-0.0097		85,502
Most-active 10 hour timing, rank-normalized	SLEEP AND CIRCADIAN	0.0480	▼-0.0100		85,723

Source: T2D Knowledge Portal (https://t2d.hugeamp.org). Search using "rs35874116" variant. Phenotypic traits with p<0.05 are shown.

Supplemental Methods

Plasmids

Sequences for human TAS1R2 and TAS1R3 with extracellular FLAG and c-myc tags, respectively, were previously cloned into pCEP4 (Invitrogen) (1) and the plasmids are deposited with Addgene under numbers 113945 and 113948. The Ile191Val mutation was introduced into TAS1R2 by overlap extension PCR and the mutated sequence was confirmed by Sanger sequencing. For measuring calcium signaling, pCEP4-FLAG-TAS1R2 was co-transfected with untagged human TAS1R3 and Gα16-gust44 cloned into pEF-DEST51 (2).

Calcium responses

Functional expression: As described previously (3, 4), HEK293 cells were cultured in Dulbecco's modified Eagle's medium supplemented with 10% fetal bovine serum at 37 °C under a humidified atmosphere containing 5% CO_2. Cells were seeded onto a 35 mm recording chamber (ibidi, Martinsried, Germany). After 24 hour-incubation, HEK293 cells were transiently cotransfected with T1Rs and Ga16-gust44 (0.9 μg each) using Lipofectamine™ 2000 transfection reagent (Thermo Fisher Scientific, Massachusetts, USA) (2.5 μl per 0.9 μg DNA). Ca^{2+} imaging assays were performed 24 hours after transfection.

Single-cell Ca^{2+} imaging: Transfected cells in 35 mm recording chambers were loaded with 3.0 mM fluo-4 acetoxymethyl ester (Thermo Fisher Scientific) for 30 min at 37 °C and washed by Hank's balanced salt solution (HBSS) (Thermo Fisher Scientific) containing 10 mM 4-(2-hydroxyethyl)-1-piperazineethanesulfonic acid (HEPES) (pH 7.4). The dye-loaded cells were subjected to Ca^{2+} imaging. A bath perfusion system was used for the determination of the activation kinetics. Taste solutions diluted in HBSS containing 10 mM HEPES were applied sequentially to the cells for 25 s with a peristaltic pump at a flow rate of 1.0 ml/min. Fluorescent images were obtained using an S Fluor 620/0.75 objective lens (Nikon, Tokyo, Japan) via a cooled-CCD camera (C6790, Hamamatsu Photonics K.K., Shizuoka, Japan) fitted to a TE300 microscope (Nikon). AquaCosmos software (v. 1.3, Hamamatsu Photonics) was used to acquire

and analyze fluorescent images. A 5 min interval was maintained between each tastant application to ensure that the cells were not desensitized due to the previous application of taste solutions. Responses were measured from individual responding cells. Cells that repeatedly showed intracellular calcium increase to the sweet solution were counted as responding cells.

Reagents: Taste substances were dissolved in HBSS containing 10 mM HEPES. Chemical compounds used in this study were aspartame (0.03, 0.1, 0.3, 1, 3, 10, 30 mM) and sucrose (10, 30, 100, 200 mM) as sweet taste stimuli. Regents were purchased from Ajinomoto Co., Inc., Tokyo, Japan (aspartame), and FUJIFILM Wako Pure Chemical Corporation, Osaka, Japan (sucrose).

Data Analysis: In the analysis of single-cell responses, changes in $[Ca^{2+}]_i$ were monitored as changes in fluo-4 fluorescence. Fluorometric signals are expressed as relative fluorescence changes: $\Delta F/F_0 = (F-F_0)/F_0$, where F_0 denotes the baseline fluorescence level. The magnitude of the calcium increases from 5 to 25 s after stimulus onset was measured and averaged. The data were expressed as the mean ± S.E. of the $\Delta F/F_0$ value. EC50 values were calculated from individual dose-dependent-response data using curving-fitting routines of Origin 5.0 (Microcal Software).

Surface and total expression of TAS1R2/TAS1R3

Cell culture and transfection: Expi293F cells were cultured in Expi293 expression medium (ThermoFisher Scientific) at 37 °C with a humidified atmosphere containing 8% CO_2. For 1-ml transfections, 1 μg plasmid DNA was prepared in 50 μl OptiMEM (Gibco). If two plasmids were co-transfected, then 500 ng of each plasmid were mixed. 2.7 μl ExpiFectamine 293 reagent (ThermoFisher Scientific) was prepared separately in 50 μl of OptiMEM and, after 5 min incubation at room temperature, DNA and ExpiFectamine 293 solutions were combined and further incubated for 30 min. Total 100 μl of transfection reagent mixture was added to 1 ml of 2 $\times$ 10^6 cells.

Flow cytometry analysis: Transfected cells were collected 22–27 h post-transfection by centrifugation at 500 x *g,* 1 min. The cell pellet was resuspended in 800 μl of cold phosphate-buffered saline (PBS) containing 0.2% bovine serum albumin (PBS-BSA) and then split into two tubes for staining surface and whole-cell protein. For surface staining, cells were centrifuged, resuspended in 40 μl PBS-BSA containing 1/133 dilution of antibodies (anti-FLAG–Cy3 clone M2 from Sigma and anti-c-Myc–Alexa Fluor 647 clone 9B11 from Cell Signaling), and incubated for 20 min on ice in the dark. Cells were washed twice with 800 μl of PBS-BSA, resuspended in 300 μl of PBS-BSA, and analyzed. For whole-cell protein staining, BD Cytofix/Cytoper Fixation/Permeabilization kit (BD Biosciences) was used. Cells were centrifuged and resuspended in 250 μl of Fixation/Permeabilization solution for 20 min on ice in the dark. Cells were washed twice with 1 ml of 1× BD Perm/Wash buffer and 0.5× PBS–BD Perm/Wash buffer, and resuspended in 40 μl of wash buffer. 0.3 μl of antibody was then added. Samples were incubated for 30 min on ice in the dark, washed twice with 250 μl of wash buffer, and resuspended in 250 μl of wash solution for analysis. Surface and total expression of TAS1R2 and TAS1R3 were measured on a BD LSR II or BD Accuri C6 (BD Biosciences). The data were collected using BD FACSDiva software (BD Biosciences) and analyzed using FCS Express 6 (De Novo Software). Gates were set on negative controls with 0.5% of events falling within the gate. Percentages of fluorescence-positive cells were determined.

Fluorescence resonance energy transfer (FRET) microscopy

Time-correlated single photon counting (TCSPC): Time-correlated single photon counting data acquisition was performed as previously described (5, 6). TCSPC histograms were obtained using HEK AAV-293 cells expression mCyRFP1-TAS1R2 WT/I191V alone or co-expressing mCyRFP-TAS1R2 WT/I191V with mMaroon1-TAS1R3 as described in the experimental protocol. Fluorescently labeled proteins were manually selected using 200 mm focal length planoconvex lens in a flip mount to defocus the excitation supercontinuum laser beam (Fianium) to excite the

whole cell. To excite mCyRFP1, the excitation laser beam was filtered through 482/18 nm bandpass filter and 0.5 neutral density filter, and emitted fluorescence was detected using 640/50 nm bandpass filter. After selection of a cell for spectroscopy, the defocusing lens was removed from the light path, the laser intensity was attenuated with a 1.0 neutral density filter, and the laser focus was positioned on a region of the cell that yielded a fluorescence intensity of 100,000 photons/s. Under these excitation conditions, we observed less than 5% photobleaching during the acquisition period. Fluorescence was detected through a 1.2 N.A. water-immersion objective with avalanche photodiode and photon counting module (PicoHarp300, PicoQuant, Germany) using a time channel width of 16 ps. 60 s of acquisition was performed for each cell, excluding cells that showed significant fluorescence intensity changes due to movement. Under these conditions, the donor-only decay was single-exponential (χ^2 ranging from 1.02 to 1.18 for mCyRFP1-TAS1R2 WT and χ^2 ranging from 1.06 to 1.32 for mCyRFP1-TAS1R2 I191V). In cells expressing donor- and acceptor-labeled proteins, additional shorter lifetimes were observed, which we attributed to FRET. Fluorescence decay histograms were analyzed using global analysis in SymPhoTime 64 software with fixed lifetime for donor alone (3.35 ns) and freely variable lifetimes and amplitudes for all lifetimes. Analysis of distribution of receptors in dimer complexes in Figure 2B was performed using global analysis with shared lifetime and freely variable amplitude for FRET species. The percentage of receptors that were in the dimer complexes was calculated from the amplitudes of the donor alone and amplitude of the FRET component according to the relationship: Receptors in dimer complexes (%) = $100\times(A_{FRET}/A_{DONOR}+A_{FRET})$, where A_{DONOR} and A_{FRET} are pre-exponential factors (amplitudes) obtained from a 2-exponential fit. The intrinsic FRET efficiency of the population of donors that were in dimer complexes was calculated according to the relationship: FRET Efficiency (%)=(1-τ_{DA}/τ_D), where τ_D is lifetime of the donor alone and τ_{DA} is lifetime of the donor in the presence of acceptor..

Cloning: mCyRFP1-C1 (7) vector and the pcDNA3.mMaroon1-C1 (8) were obtained from Addgene. Human TAS1R2 WT or TAS1R2 I191V was fused to the C-terminus of mCyRFP1. mMaroon1 was amplified from the pcDNA3.1 vector using the polymerase chain reaction and inserted into YFP-C1 (9) in place of the YFP fluorescent tag. The sequence for human TAS1R3 was inserted into mMaroon1 vector to create an mMaroon1-TAS1R3 fusion construct. The full sequence of all constructs was verified by DNA sequencing.

Cell culture and transfection: HEK AAV-293 cells were cultured using DMEM medium (Corning, Mediatech Inc., Manassas, VA) supplemented with 10% fetal bovine serum (FBS) in humidified CO_2 incubator. Subsequently, the plasmids pcDNA3.1-mMaroon1-TAS1R2 (WT or I191V) and pcDNA3.1-mCyRFP1 were co-transfected into HEK AAV-293 cells using Lipofectamine 3000 Transfection kit (Invitrogen, Life Technologies Corp., Carlsbad, CA) and transferred into DMEM with 10% FBS and 2% DMSO (Sigma). 48 hours post-transfection the cells were trypsinated (ThermoScientific, Waltham, MA) and plated into sterile glass bottom chamber slides and incubated for at least one hour before imaging. The media in all experiments was washed out and replaced by PBS (Corning, Mediatech Inc., Manassas, VA) immediately before imaging.

Ligands: To investigate the effect of 10 mM aspartame (Sigma), the cells were transiently transfected as described above and trypsinated 24 hours post-transfection and transferred into DMEM with 1 g/L glucose (Corning, Mediatech Inc., Manassas, VA) supplemented with 10% FBS and 2% DMSO and incubated for another 24 hours. Glucose-starved cells were imaged before and 10 minutes after aspartame addition.

Clinical studies

For cross-sectional study NCT02835859 we recruited healthy lean participants as described in (10). All participants were retrospectively assigned to two groups based on TAS1R2 genotypes. Recruitment, enrollment and all study-related visits, including specimen collection and point-of-care laboratory testing, took place at Advent-Health Translational Research Institute (TRI) Clinical Research Unit (CRU). The study was approved by the Institutional Review Board at Advent-

Health and all participants signed an informed consent. All testing was performed after an overnight fast. Anthropometric measures (weight, height, waist circumference) were obtained with the subjects in a light hospital gown according to standardized protocols.

Oral Glucose Tolerance Test (OGTT): After fasting samples were collected (t = -10, 0 min), subjects consumed a flavored 300 ml 75 g glucose drink within 5 minutes. Blood samples were collected at 30 min increments for 2 hours thereafter or as shown in Fig.2 and in (10). Blood was collected in K2EDTA tubes with a cocktail of protease, esterase and DPP-IV inhibitors (BDTM P800 blood collection system; BD Bioscience, CA). Glucose concentrations were measured by a point of care device (NOVA StatStrip Meter); insulin, C-peptide, total GLP1, and glucagon concentrations by immunoassay (Milliplex Map Kit, Millipore, MA).

OGTT mathematical modeling and Calculations: Beta-cell function, insulin sensitivity and insulin clearance were estimated exactly as described in (11).

Fecal Microbiota: Genomic DNA was isolated from mouse and human feces using QiaAmp DNA stool kit (QIAGEN), with an additional step of bead beating for 5 min with 0.1 mm beads to ensure maximum lysis of bacterial cells. Multiplexed libraries were prepared according to the protocol from Illumina using V3-V4 region of 16S rRNA and HiFi HotStart DNA Polymerase (Kapa Biosystems) for amplification. Final amplified products were quantified by ABI Prism library quantitation kit (Kapa Biosystems). Each sample was diluted to 10 nM, and equal volume from each sample was pooled. The quality of the library was checked by Bio-Rad Experion bioanalyzer (Bio-Rad). Illumina MiSeq platform was used for sequencing (Novogene Bioinformatics Technology Co., Ltd). Raw FASTQ sequences were quality checked with FastQC v0.11.5. Raw sequences were trimmed with ‘cutadapt’ v2.6 to remove low quality bases and adaptor sequences. The trimmed FASTQ files were converted into a Qiime2 v2019.1 file format. The imported forward and reverse reads were merged using ‘vsearch’ with a minimum sequence length of 200 base pairs. Joined pairs were quality trimmed using Qiime2 ‘quality filter’ with an average quality score of 20 (Q20) over a 3 base pair sliding window and removing trimmed reads

having less than 75% of their original length. ‘Deblur 16S rRNA positive filter’ was used as a final quality control step by dereplicating and removing chimera sequences from each sample; reads were trimmed to a final length of 195 base pairs. Taxonomic analysis and Operational Taxonomic Unit (OTU) tables were created with Qiime2 using 100% sequence identity threshold (12) and converted using biom format. The median sequencing depth for human samples was 51,274 reads and for mouse samples 48,561 reads. To avoid bias of sequencing depth, the OTUs were filtered for singletons and rarefied to lowest sample depth (39,895) resulting in a Good’s coverage index >99.98% for all human or mouse samples. (MicrobiomeAnalyst.ca (13)). Next, alpha diversity was calculated using the following indices: Chao1 (species richness), Shannon and Simpson (species richness and evenness) (14, 15) (MicrobiomeAnalyst.ca). Next, OTUs with very small counts (<4) in very few samples (<20% prevalence) were filtered out from all subsequent analysis (13). For beta diversity analysis, Bray-Curtis dissimilarity was calculated using the R package Vegan (16). The dissimilarity matrix was ordinated using Nonmetric Multidimensional Scaling (NMDS) and the between-subject beta diversity was tested for statistical significance with permutational Multivariate ANOVA (PERMANOVA, Adonis) (17).

References (for Supp. Methods only)

1. Park J, Selvam B, Sanematsu K, Shigemura N, Shukla D, and Procko E. Structural architecture of a dimeric class C GPCR based on co-trafficking of sweet taste receptor subunits. *The Journal of biological chemistry.* 2019;294(13):4759-74.
2. Shigemura N, Shirosaki S, Sanematsu K, Yoshida R, and Ninomiya Y. Genetic and molecular basis of individual differences in human umami taste perception. *PloS one.* 2009;4(8):e6717.
3. Sanematsu K, Kitagawa M, Yoshida R, Nirasawa S, Shigemura N, and Ninomiya Y. Intracellular acidification is required for full activation of the sweet taste receptor by miraculin. *Sci Rep.* 2016;6:22807.
4. Sanematsu K, Kusakabe Y, Shigemura N, Hirokawa T, Nakamura S, Imoto T, et al. Molecular mechanisms for sweet-suppressing effect of gymnemic acids. *The Journal of biological chemistry.* 2014;289(37):25711-20.
5. Bovo E, Nikolaienko R, Cleary SR, Seflova J, Kahn D, Robia SL, et al. Dimerization of SERCA2a Enhances Transport Rate and Improves Energetic Efficiency in Living Cells. *Biophysical journal.* 2020;119(7):1456-65.
6. Blackwell DJ, Zak TJ, and Robia SL. Cardiac Calcium ATPase Dimerization Measured by Cross-Linking and Fluorescence Energy Transfer. *Biophysical journal.* 2016;111(6):1192-202.

7. Laviv T, Kim BB, Chu J, Lam AJ, Lin MZ, and Yasuda R. Simultaneous dual-color fluorescence lifetime imaging with novel red-shifted fluorescent proteins. *Nature methods.* 2016;13(12):989-92.
8. Bajar BT, Lam AJ, Badiee RK, Oh YH, Chu J, Zhou XX, et al. Fluorescent indicators for simultaneous reporting of all four cell cycle phases. *Nature methods.* 2016;13(12):993-6.
9. Hou Z, and Robia SL. Relative affinity of calcium pump isoforms for phospholamban quantified by fluorescence resonance energy transfer. *J Mol Biol.* 2010;402(1):210-6.
10. Serrano J, Smith KR, Crouch AL, Sharma V, Yi F, Vargova V, et al. High-dose saccharin supplementation does not induce gut microbiota changes or glucose intolerance in healthy humans and mice. *Microbiome.* 2021;9(1):11.
11. Karimian Azari E, Smith KR, Yi F, Osborne TF, Bizzotto R, Mari A, et al. Inhibition of sweet chemosensory receptors alters insulin responses during glucose ingestion in healthy adults: a randomized crossover interventional study. *The American journal of clinical nutrition.* 2017;105(4):1001-9.
12. Edgar RC. Updating the 97% identity threshold for 16S ribosomal RNA OTUs. *Bioinformatics.* 2018;34(14):2371-5.
13. Chong J, Liu P, Zhou G, and Xia J. Using MicrobiomeAnalyst for comprehensive statistical, functional, and meta-analysis of microbiome data. *Nat Protoc.* 2020;15(3):799-821.
14. Kim BR, Shin J, Guevarra R, Lee JH, Kim DW, Seol KH, et al. Deciphering Diversity Indices for a Better Understanding of Microbial Communities. *J Microbiol Biotechnol.* 2017;27(12):2089-93.
15. Morris EK, Caruso T, Buscot F, Fischer M, Hancock C, Maier TS, et al. Choosing and using diversity indices: insights for ecological applications from the German Biodiversity Exploratories. *Ecol Evol.* 2014;4(18):3514-24.
16. Dixon P. VEGAN, a package of R functions for community ecology. *J Veg Sci.* 2003;14(6):927-30.
17. Anderson MJ. A new method for non-parametric multivariate analysis of variance. *Austral Ecol.* 2001;26(1):32-46.